

Stretchable Circuits and Sensors for Robotic Origami

Jamie K. Paik, Rebecca K. Kramer and Robert J. Wood, *Member, IEEE*

Abstract—Programmable materials based on robotic origami have been demonstrated with the capability to fold into 3D shapes starting from a nominally 2D sheet. This concept requires high torque density actuators, flexible electronics and an integrated substrate. We report on two types of stretchable circuitry that are directly applicable to robotic origami: meshed copper traces and liquid-metal-filled channels in an elastomer substrate. Both methods maintain conductivity even at large strains (during stretching) and curvatures (during folding). Both circuit designs are integrated with a tiled origami module actuated by a shape memory alloy actuator. We also integrate a soft curvature sensor into the robotic origami module that measures the full range of motion of the module in real-time.

I. INTRODUCTION

Robotic origami refers to a reconfigurable robot that folds into various 3D shapes from its initial flat configuration. The system consists of a network of tiles connected with compliant joints and folding actuators. The tiled body is composed of flexible and rigid sections that enable the robot to attain arbitrary shapes [1]. The reproducible shape formation results from individually actuated folding edges and the same technology can apply to millimeter and sub-millimeter scale robots that require high torque to weight ratio and form factors. Novel fabrication methods are needed to build and integrate actuators, electronics, and a multi-material body as seen in the robotic origami in Fig. 1 [2].

The current choice of folding actuator is a custom shape memory alloy (SMA) sheet machined and annealed into a torsional actuator [3]. The low profile of the SMA torsional actuator conforms to the initial and final shape the robot. However, to accommodate compound folds [2] of the structure (i.e. folds several layers thick), elastic joints that can both bend and stretch are critical for the creation of complex topologies. This is a significant challenge given the strain limits of bulk metals and the poor conductivity of conductive polymers, inks, and composites. Here we explore two prototype methods: micro-patterned copper-mesh composites and liquid-metal-filled-microchannels. This paper compares and contrasts these solutions to elastic circuits that are compact, thin, and enable power and signal interconnection between components of robotic origami. Furthermore, these techniques may be expanded to a variety of millimeter-scale robots where conformable electronics or sensors are required. This work reviews the current electrical properties and methods of fabricating flexible electronics and circuits (Section II), and presents the design and fabrication process

of the two different circuits (Section III) and their integration to a single origami tile module (Section IV and V). Experimental realization of the stretchable circuits are described, including the application of a curvature sensor for proprioceptive feedback in the folding joints (Section VI).

II. RELATED WORK IN FLEXIBLE ELECTRONICS AND CIRCUITS

Robotic origami requires unique engineering solutions for actuation, rigid and flexible body materials, and stretchable electronics. For small-scale robots, limited real estate on the robot body requires electronics to conform to packages that may not be flat or static. Also, robots with soft components and moving structures, such as robotic origami, will benefit from stretchable circuits and electronics, which do not impede the motion of the host structure and remain functional even when significantly stretched ($2\times - 10\times$).

In one example, Rogers' group used patterned thin silicon nanoribbons and membranes to introduce flexibility in a silicon substrate or thin metal film [4], [5], [6]. However, since these techniques rely on integrated circuit fabrication, scaling up beyond a few tens of centimeters could be challenging. As an alternative to buckled films, liquid-metal-filled polymer channels have been studied. Examples include eutectic gallium indium (eGaIn)-filled RF antennas [7] and soft pressure sensors [8] that showed promising results as compliant electrical devices. In [9], the authors suggest different ways of using eGaIn and other liquid metals for flexible electronics. However, no experimental data has yet been presented. Numerous groups also have achieved preliminary results in flexible memory using organic materials, as well as two-electrode devices based on thin films of titanium dioxide and graphene. Graphene, a single sheet of graphite, has shown applicability as a flexible transistor material faster than silicon transistors [10]. Another material, molybdenite, is also comparable to graphene as a single layer with similar electrical and optical properties [11]. There are printable electronics using carbon nanotubes or various nanowires made of semiconductors. Printable circuits on various flexible polymers and materials, such as paper, have also been presented [12]. Moreover, studies on electrical transport in semiconductor nanowires and nanocontacts suggest possible applications in sub-millimeter scale circuit traces required for robotic origami. However, the impact of wire diameter, doping level, surface treatment, contact metal, and substrate material is vital to the design and operation of devices and may limit the scope of applications [13]. Also, in comparison to metals, semiconductors have nine orders of magnitude higher electrical resistivity. For transistors and memory chips,

The authors are with the Microrobotics Laboratory of the School of Engineering and Applied Sciences, Harvard University, Cambridge, MA 02138 jpaik@seas.harvard.edu

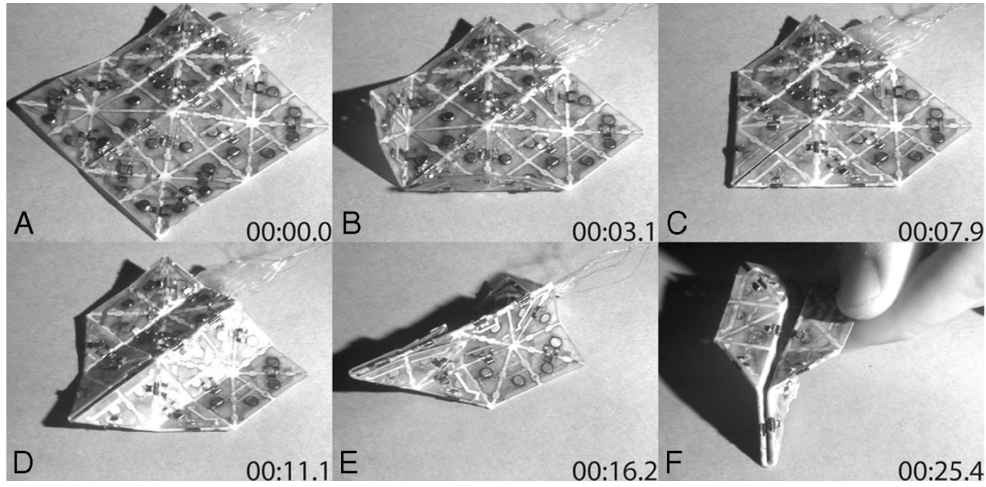


Fig. 1. 32-tile self-folding sheet, capable of achieving two distinct shapes [2]: a “paper airplane” and a “boat”. Flat sheet prior to folding (A). Four-actuator group controlling flaps activated (B). Magnets for the first fold engaged (C). Remaining actuators are activated (D). Final shape (E) and inverted (F).

lower conductivity of semi-conductors is not critical; but for a circuit path that requires high current densities, this could limit the applicability.

In this paper we describe two flexible circuits that power SMA actuated modules (which require relatively large currents). These circuit designs do not require a clean room nor extensive fabrication processes, yet display high electrical conductivity while being highly stretchable for robotic origami and related soft robotics applications.

III. STRETCHABLE CIRCUITS

The robotic origami requires highly stretchable circuitry that expands as well as bends along folding edges (when folded multiple times, the elongation strain can exceed 100%). We present two different solutions to stretchable circuitry that have relatively simple fabrication processes and are easily modifiable to different circuit requirements and geometries. Each technique results in a in circuits with low profile (sub-millimeter) and can be “printed” as an independent circuit layer onto the substrate.

A. Patterned Metal Circuits

One solution for a stretchable circuit involves creating a transversely deformable pattern in a metal trace. We start with a copper/polyimide composite ($40\mu\text{m}$ thick copper and $30\mu\text{m}$ thick polyimide) used for conventional flex-circuit fabrication. We create a mesh pattern in the sections of the traces that experience the most strain. This pattern is made of slits orthogonal to the long axis of the trace, and stacked with variable overlap along the trace direction. While keeping the gap, the row clearance, and the slit length constant, we varied the “phase shift” as defined in Fig. 2(a).

We constructed six COMSOL models that have a slit phase shift of 0, 25, 51.5, 65.5, 75 and 100%. Each model was stretched at 220MPa . Figure 2(b) shows a representation of a deformed shape and Fig. 3 displays their overall elongation and peak stress. The simulation shows increasing strain and

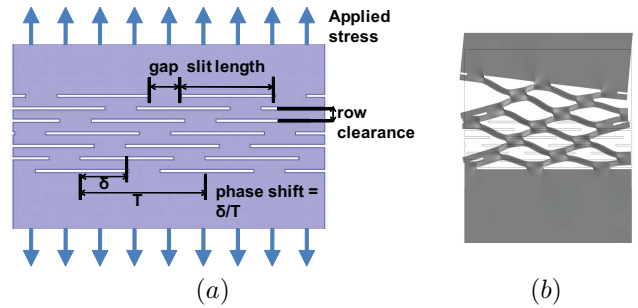


Fig. 2. Description of slit design parameters (a), COMSOL model of a deformed slit (b).

stress with an increase in the phase shift. We can regard this trend as a result of basic beam theory, where longer beams produce higher deflection in the overall mesh. However, the 100% phase shift sample shows a decrease in flexibility which can possibly be explained by the symmetry in the architecture, which distributes the stress and counteracts elongation. We choose the slit pattern with 75% phase shift ($40\mu\text{m}$ row clearance, $100\mu\text{m}$ gap, and $300\mu\text{m}$ slit) that has the highest elongation, and thus greatest compliance to stretching, to design the circuit. The chosen slit pattern is tested in Section VI.

In order to produce the circuit layer, the copper side of the sheet is covered with a positive photoresist (Shipley SP 24D) and cured. The outline of the circuit is dry etched by raster-machining the area with a diode-pumped solid state (DPSS) micro-machining laser to expose the resist layer. When submerged in ferric chloride, the exposed area etches to leave only the polyimide substrate. Once rinsed thoroughly with water, the circuit is laser machined to create meshes in the sections of the traces that will experience the highest axial strains, according to the analysis described above. It is important to post-process the meshes, as the wet-etching process can be aggressive and less controllable given the

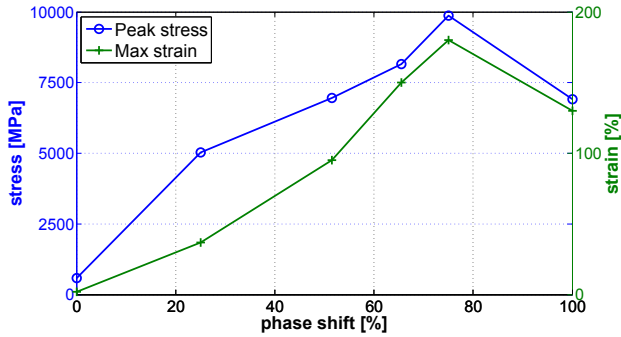


Fig. 3. Impact of varying phase offset slit patterns on the peak stress and strain of the copper-mesh circuit. Comparison of six COMSOL models.

relatively high aspect ratio and fine feature sizes required for the mesh patterns. When the pattern is complete, the whole circuit is cleaned with acetone to remove cured photoresist and finally rinsed with water to be used as a circuit layer. The final circuit layer is embedded into the tiled structure of the robotic origami, which is described in Section IV.

B. eGaIn-Filled PDMS Micro-channel Circuit

Liquid-metal-filled micro-channels in polymer substrates are also a viable option for flexible circuits. The flexible circuit is composed of thin sheets of polydimethylsiloxane (PDMS, Dow Corning) silicone rubber embedded with conductive liquid microchannels of non-toxic eutectic gallium-indium (eGaIn, BASF). Microchannels are fabricated by casting liquid PDMS elastomer onto a glass mold that is patterned with adhesive-backed polyimide film. The polyimide film is adhered to a clean glass slide (Electron Microscopy Sciences) and the outline of the desired circuit pattern is transferred to the film via a laser micro-machining system (VersaLaser, Universal Laser Systems). After patterning, excess film is peeled away, and the pattern is rinsed with isopropyl alcohol and deionized water to remove unwanted residue. In order to discourage bonding between silicon rubber and the mold in subsequent steps, a hydrophobic monolayer of trichloro(1H,1H,2H,2H-perfluorooctyl)silane (Aldrich) is introduced to the glass surface through vapor deposition.

PDMS is spin-coated in liquid form (10:1 mass ratio of elastomer base to curing agent) onto the mold to result in a thin elastomer film of tunable thickness. Similarly, PDMS is also cast onto an unpatterned glass slide or silicon wafer, which results in an unpatterned elastomer film. Microchannels are constructed by bonding layers of patterned PDMS to unpatterned PDMS via oxygen plasma treatment (Technics Plasma Stripper/Cleaner; 65 W for 30 s). The microchannels are filled with eGaIn using a syringe dispensing method developed for thin elastomer sheets, as outlined in [14]. Finally, wire is inserted into the ends of the microchannels, which are then sealed with a drop of uncured PDMS.

The flexible eGaIn circuit shown in Fig. 4 is approximately $300\mu\text{m}$ in total thickness. Each PDMS layer (patterned and

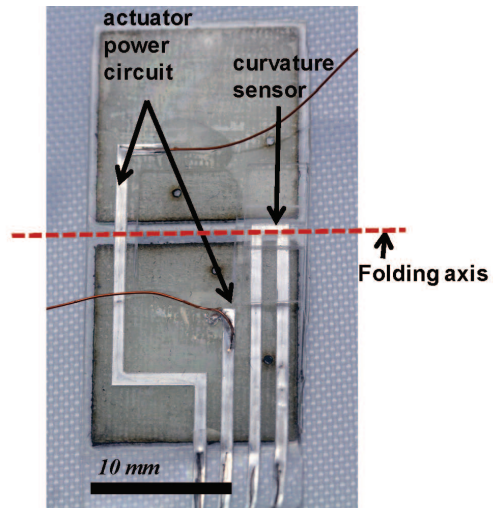


Fig. 4. Fully integrated stretchable electronics on a origami tile module: eGaIn-filled circuitry and a curvature sensor.

unpatterned) is about $150\mu\text{m}$ thick, which corresponds to a spin-rate of 467 rpm on glass and 511 rpm on a silicon wafer. Note that these values were obtained for one particular spin-coater and may vary for different machines. The polyimide film used is $50\mu\text{m}$ in thickness, and the microchannels are 1mm in width.

The elasticity of the circuit may be tuned by choice of material. For example, PDMS has an elastic modulus of 1-2 MPa, while EcoFlex silicon rubber (0030, SmoothOn) is considerably more compliant with a Young's modulus close to 125 kPa.

IV. ACTUATION AND ORIGAMI SUBSTRATE

To test the adaptability of the stretchable circuits for use in self-folding sheets, we apply the two circuits to an actuated module. The actuator consists of an annealed SMA actuator and a heater [3]. The actuator module connects two adjacent tiles and applies a torque on the joint to actuate a fold. We used the SMA actuator introduced in [3] with a newly designed external heater. The heater is designed as a high resistance heating element (as opposed to Joule heating in the body of the actuator) to avoid I^2R losses in the circuit path. A specific heater pattern has been designed on a nickel alloy sheet (Dupont Kapton KH), which is dry-etched and wet-etched to construct the heater, and then insulated and attached to the SMA actuator. The test prototype has a rapid heating rate as discussed in Section VI. Figure 5 illustrates the actuator module and its actuation configuration. The z-shaped actuator, shown in Fig. 6, produces a torque about the folding axis upon activation with a blocked torque of up to 3.5mNm .

For an origami prototype capable of generating multiple shapes, a large set of tiles is needed. In this paper, we demonstrate the functionality and adaptability of the stretchable circuits with a single set of modules composed of two square tiles. The s-glass tiles are made of resin cured glass-fiber that is layered to have a cured thickness of $300\mu\text{m}$. After

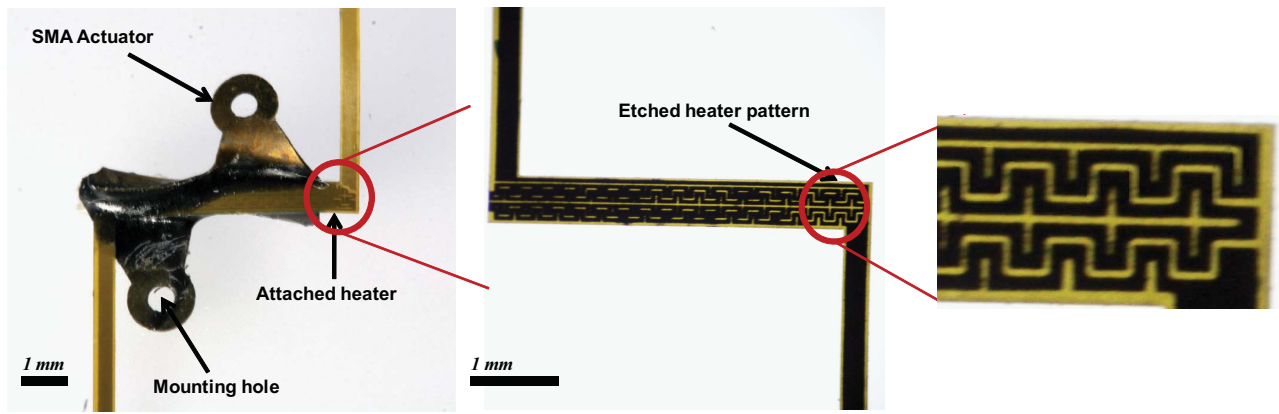


Fig. 6. Actuator module with an external heater. Insets show the custom designed micro-heater and its etched pattern.

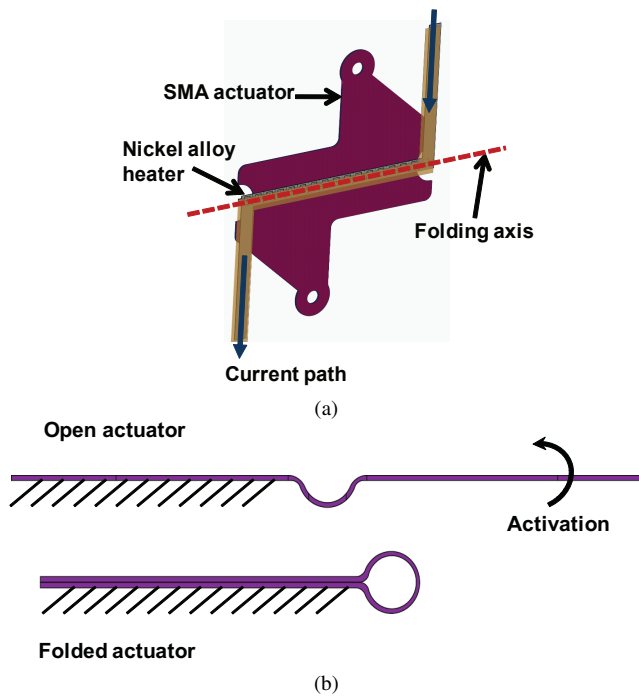


Fig. 5. Illustrations of the complete actuator module (a) and its configuration before and after actuation (b).

laser machining desired planform shape including actuator attachment features, the excess material is removed while the tiles remain temporarily bonded on a backing to maintain relative positions. The tiles are covered with a thermoplastic polyurethane elastomer ($76\mu\text{m}$ American Polyfilm 70 shore A, polyether polyurethane), vacuum bagged, and put in an oven (140°C for 30 min). The vacuum bag ensures bonding between the s-glass surface, folding edges, and the rest of the exposed area. The bonded s-glass tiles can be carefully removed from the backing. For copper-mesh circuits, the circuit layer is directly placed onto the s-glass side before polyurethane covering. The polyurethane layer infuses into the delicate patterns to protect the circuit layer. When the copper-mesh circuit is layered on the newly exposed s-glass side, the tackiness from the removed backing keeps

the circuit layer in position. Once the remaining side is covered with a polyurethane layer, it is again vacuum bagged and cured. In this way, each copper-mesh is coated with polyurethane such that when stretched, the polymer between the slits brings the deformed mesh structure back into the unstretched position. In the case of eGaIn-filled channels, PDMS is bonded directly to the s-glass substrate. The s-glass substrate must first be cleaned but requires no second polyurethane layer.

V. MODULE INTEGRATION

In order to bond the surface of the s-glass tiles and the PDMS structures (both circuit and curvature sensor), the surfaces of the PDMS flexible circuits and the s-glass tiles are bonded together through an amino-epoxy chemical bonding method [15], [16]. Both surfaces are first cleaned and exposed to oxygen plasma (65W for 30s). Immediately following plasma exposure, the PDMS surface to be bonded is coated in 5% (v/v) (3-Aminopropyl)triethoxysilane (99% Sigma Aldrich), and the s-glass surface is coated in 5% (v/v) (3-Glycidyloxypropyl)trimethoxysilane (98% Sigma Aldrich). After at least 20 minutes of silane immersion, excess silane is discarded and the pieces are placed on a hot plate at 50°C . When the surfaces are dry, they are brought into contact with light pressure. Placing the bonded surfaces in an oven at 60°C for several hours finalizes the chemical bond between the flexible circuit and s-glass tiles.

Integration of the actuator module and completed tiles is accomplished mechanically using miniature bolts with a thread diameter of 0.5mm . The excess length of the bolt is trimmed and thread-locked using cyanoacrylate (Loctite 416). The electrical connection of the ends are soldered to either to the electrode pads of the copper circuit (exposed sections in the polyurethane) or to the wire outlets of the eGaIn circuit.

Figure 7 shows the completely integrated stretchable circuits of both copper-mesh design and eGaIn-filled channel designs. For the eGaIn-based circuit, we also added a soft curvature sensor alongside the actuator, for which the measurements are discussed in the following section.

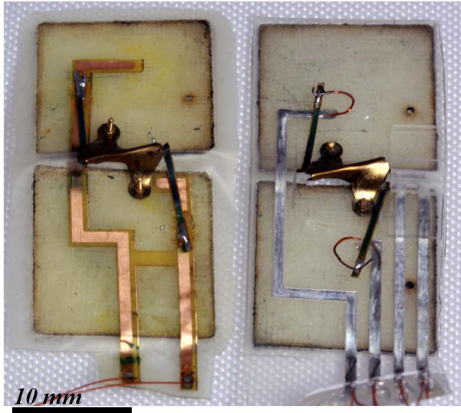


Fig. 7. Two flexible circuits integrated with origami tile modules. The left shows the copper-mesh circuit and the right is the eGaIn circuit. Both circuits have trace widths of 1mm . For the eGaIn circuit, the curvature sensor is embedded to the right of the actuator.

VI. EXPERIMENTS AND DISCUSSIONS

The prototype stretchable circuits were tested for maximum operating strain and the ability to transfer power to the actuators during folding of the robotic origami. We also verified the applicability of a compliant curvature sensor to measure fold angle.

A. Strain Testing

In order to determine the strain limits for both circuits, we performed a stress-strain test while observing both electrical and mechanical failure. An Instron materials testing system grips two ends of a specimen and moves at a constant rate in tensile mode to measure the applied load (see Fig. 8). Five samples of each circuit are wired to a multimeter to measure the conductivity while they were stretched to failure. Copper-mesh samples (1mm wide, 0.075mm thick) failed on average under 56% strain at a corresponding 3.02N load. When the copper-mesh width changed to 1.5mm , the strain at failure increased to 100%. The eGaIn-filled PDMS samples with channels 1mm wide had an average of 162% strain-at-failure under 17.6N loading. Here, failure is defined as either mechanical fracture or electrical open circuit. Both stretchable circuit types displayed continuous conductivity until mechanical fracture. The copper-mesh circuit failed when the meshing broke completely within the polyurethane covering; with a finer mesh design or a wider section, the copper-mesh circuit could potentially endure greater strains. The eGaIn circuit maintained conductivity until the PDMS structure and channel failed (ruptured) mechanically. The copper-mesh circuit maintained a relatively constant electrical resistivity during elongation (from 0.22Ω to 0.24Ω) while the eGaIn circuit experiences a greater resistance change before it fails (from 0.67Ω to 1.08Ω). For the origami tile circuits that power the SMA actuator, we choose 1.0mm wide circuit path for both circuit types.

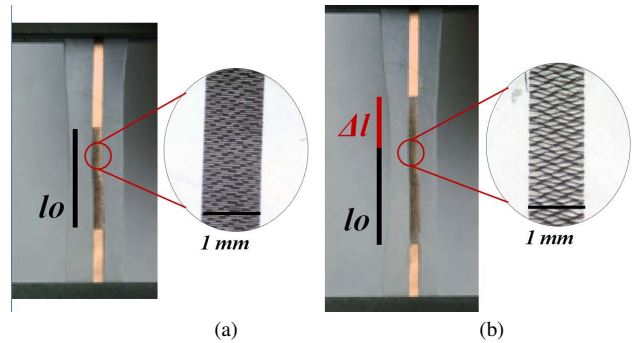


Fig. 8. A sample of the polyurethane covered copper-mesh circuit placed in an Instron Material Testing system. The insets show the magnified views of the mesh that is in the neutral position (a), and elongated to the point of failure (b).

TABLE I
PERFORMANCE COMPARISON FOR COPPER-MESH AND eGaIn
CIRCUITS.

	Copper-mesh circuit	eGaIn circuit
Range of motion	$0-180^\circ$	$0-180^\circ$
Mass (without tiles)	0.063 g	0.065 g
Actuation time constant	≈ 1 s	≈ 1 s
Power consumption (no load)	0.092 W	0.187 W
Strain to failure	56%	162%
Trace resistivity change	$0.22\Omega - 0.24\Omega$	$0.67\Omega - 1.08\Omega$

B. Actuation

To evaluate the functionality of both circuit types for robotic origami, the devices shown in Fig. 7 are actuated while observing folding range, time to fold, and power consumption (Fig. 9). Both the copper circuit and the eGaIn circuit displayed similar responses to folding actuation, but the eGaIn circuit required more power (average power for a full range of motion without external load) to reach the same range of motion with the test module (see Table I). This larger power consumption is due to the more resistive circuit path. The copper and eGaIn-filled circuits have similar dimensions (i.e. same channel width, with $40\mu\text{m}$ thick copper and $50\mu\text{m}$ deep eGaIn channel). However, because copper is 20 times more conductive than eGaIn [17], higher I^2R losses are present in the eGaIn circuit path. (even with the difference in the depth of the circuit). Also, due to the flexible nature of the channel material, the channel geometry changes increase the circuit resistance when stretched. This property is exploited for the curvature sensor discussed in the following section.

C. Compliant curvature sensor

A compliant curvature sensor similar to the curvature sensors described in [18] is integrated with the origami module to measure deflection angle when actuated by the SMA actuators. Characterization and calibration of the sensor is necessary and conducted prior to use. To calibrate, pure bending of the sensor is induced by positioning the two s-glass tiles at specific angles. During testing, the tiles are



Fig. 9. Folding sequence of the origami module powered with the eGaIn circuit. The integrated soft curvature sensor measures the angular deflection by detecting the change in resistance, given in Ohms.

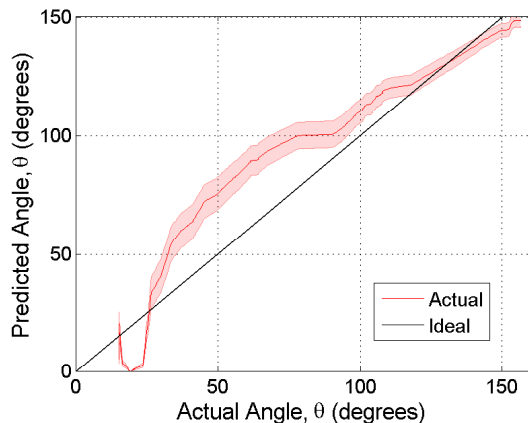


Fig. 10. A comparison between actual angle and predicted angle, based on compliant curvature sensor measurements taken over five folding sequences. The shaded error bar represents one standard deviation of the data.

attached to rigid blocks to increase positioning accuracy and eliminate any twisting or stretching of the sensor. The tiles are manually oriented from 0° to 170° , and the change in electrical resistance is measured with a precision multimeter (Fluke 8845A). As expected, the change in electrical resistance ΔR increases exponentially as a function of bending angle θ . Curvature measurements are repeated 5 times, and the data is averaged and fitted to an exponential curve.

A comparison between actual angle and sensor-measured angle during actuation of the joint for a typical folding sequence is shown in Fig. 10. Actual angle is determined via motion tracking using ProAnalyst (XCITEX) software. The predicted angle is determined by calibration and the exponential curve fit to this particular sensor. The data in Fig. 10 was collected over five folding sequences and the

shaded error bar represents one standard deviation of the data. The average standard deviation of the data is 4.41° . The quadratic mean difference between actual and predicted angle is 15.36° . The average error of the sensor is 8.53%, as given as a percent of the full-scale output of 180° .

For moderate to low bending angles, there appears to be some discrepancy. This is somewhat expected, due to the non-linear relationship between change in resistance and bending angle. Small changes in resistance may therefore translate into large fluctuations in predicted angle. However, small variations in resistance may be induced by factors other than bending, such as motion of the wires that connect the liquid microchannels to the multimeter, manual rotation of the sensor during testing and fluidic or viscoelastic effects within the sensor.

VII. CONCLUSION

We have presented two effective stretchable circuit solutions that do not require extensive fabrication processes. Using these two circuit designs, we have successfully actuated an origami tile module that is driven by a single SMA actuator module. Both circuits are readily applicable for fabrication processes that require modularized circuits with high strains (near 100%) and a low profile (sub-millimeter). Relatively simple design parameters of the circuits can be adjusted for specific design requirements. The copper-mesh circuit is appropriate for structures that require post-processing in high heat (near and above 100°C) and an extremely low-profile ($70\mu\text{m}$). The eGaIn-filled PDMS micro channel circuit design is highly effective in the applications that require much higher strain (about 160%). Complications in fabricating more complex circuits (thinner and more populated channels) are under investigation.

VIII. ACKNOWLEDGEMENTS

This work was supported in part by the Defense Advanced Research Projects Agency (DARPA) under grant W911Nf-08-1-0228 (Programmable Matter) and the Wyss Institute for Biologically Inspired Engineering.

REFERENCES

- [1] N. Benbernou, E. Demaine, M. Demaine, and A. Ovadya, "A universal crease pattern for folding orthogonal shapes," *arXiv preprint arXiv:0909.5388*, 2009.
- [2] E. Hawkes, B. An, N. Benbernou, H. Tanaka, S. Kim, E. Demaine, D. Rus, and R. Wood, "Programmable matter by folding," *Proceedings of the National Academy of Sciences*, vol. 107, no. 28, p. 12441, 2010.
- [3] J. Paik, E. Hawkes, and R. Wood, "A novel low-profile shape memory alloy torsional actuator," *Smart Materials and Structures*, vol. 19, p. 125014, 2010.
- [4] I. Jung, G. Shin, V. Malyarchuk, J. Ha, and J. Rogers, "Paraboloid electronic eye cameras using deformable arrays of photodetectors in hexagonal mesh layouts," *Applied Physics Letters*, vol. 96, p. 021110, 2010.
- [5] J. Rogers and Y. Huang, "A curvy, stretchy future for electronics," *Proceedings of the National Academy of Sciences*, vol. 106, no. 27, p. 10875, 2009.
- [6] D. Kim and J. Rogers, "Stretchable electronics: Materials strategies and devices," *Advanced Materials*, vol. 20, no. 24, pp. 4887–4892, 2008.
- [7] M. Kubo, X. Li, C. Kim, M. Hashimoto, B. Wiley, D. Ham, and G. Whitesides, "Stretchable Microfluidic Radiofrequency Antennas," *Advanced Materials*, vol. 22, no. 25, pp. 2749–2752, 2010.

- [8] Y. Park, C. Majidi, R. Kramer, P. Bérard, and R. Wood, "Hyperelastic pressure sensing with a liquid-embedded elastomer," *Journal of Micromechanics and Microengineering*, vol. 20, p. 125029, 2010.
- [9] S. Mascaro, D. Mascaro, J. Abu-Khalaf, and J. Park, "Stretchable Circuit Configuration," 2010, *US Patent App.* 12/728,814.
- [10] A. Geim, "Graphene: status and prospects," *Science*, vol. 324, no. 5934, p. 1530, 2009.
- [11] B. Radisavljevic, A. Radenovic, J. Brivio, V. Giacometti, and A. Kis, "Single-layer MoS₂ transistors," *Nature Nanotechnology*, vol. 6, no. 3, pp. 147–150, 2011.
- [12] Z. Fan, J. Ho, T. Takahashi, R. Yerushalmi, K. Takei, A. Ford, Y. Chueh, and A. Javey, "Toward the development of printable nanowire electronics and sensors," *Advanced Materials*, vol. 21, no. 37, pp. 3730–3743, 2009.
- [13] S. Vivekchand, K. Kam, G. Gundiah, A. Govindaraj, A. Cheetham, and C. Rao, "Electrical properties of inorganic nanowire-polymer composites," *Journal of Materials Chemistry*, vol. 15, no. 46, pp. 4922–4927, 2005.
- [14] R. Kramer, C. Majidi, and R. Wood, "Wearable Tactile Keypad with Stretchable Artificial Skin," in *Robotics and Automation, 2011. Proceedings. ICRA 2011. IEEE International Conference on.* IEEE, 2011.
- [15] M. Vlachopoulou, A. Tserepi, P. Pavli, P. Argitis, M. Sanopoulou, and K. Misiakos, "A low temperature surface modification assisted method for bonding plastic substrates," *Journal of Micromechanics and Microengineering*, vol. 19, p. 015007, 2009.
- [16] L. Tang and N. Lee, "A facile route for irreversible bonding of plastic-PDMS hybrid microdevices at room temperature," *Lab Chip*, vol. 10, no. 10, pp. 1274–1280, 2010.
- [17] M. Dickey, R. Chiechi, R. Larsen, E. Weiss, D. Weitz, and G. Whitesides, "Eutectic Gallium-Indium (EGaIn): A Liquid Metal Alloy for the Formation of Stable Structures in Microchannels at Room Temperature," *Advanced Functional Materials*, vol. 18, no. 7, pp. 1097–1104, 2008.
- [18] R. Kramer, C. Majidi, R. Sahai, and R. Wood, "Soft Curvature Sensors for Joint Angle Proprioception," in *Intelligent Robots and Systems, San Francisco, CA, Sept. 2011. IROS 2011. IEEE International Conference on.* IEEE, 2011.